Anal. Chem. **2009,** *81,* 105–111

Optical Waveguide Sensor Based on a Porous Anodic Alumina/Aluminum Multilayer Film

Akira Yamaguchi, Kazuhiro Hotta, and Norio Teramae*

Department of Chemistry, Graduate School of Science, Tohoku University, Aoba-ku, Sendai 980-8578, Japan

An optical waveguide sensor was fabricated by forming a multilayer film made by porous anodic alumina (PAA) and Al layers on a glass substrate. The fabricated sensor system was based on the monitoring of a waveguide coupling mode, which is sensitive to the change in the refractive index of the PAA layer caused by collection of target molecules into the pores of the PAA layer. The PAA/Al multilayer film was formed by partial anodization of an Al film deposited on the glass substrate, and the waveguide coupling mode was examined by measuring angular spectra (reflectivity dependence on the incident angle of monitoring light; green He−Ne laser, 534.5 nm). A deep and sharp waveguide coupling dip was obtained for the PAA/Al multilayer system where the thicknesses of the PAA and Al layers were 200 and 17 nm, respectively. The optical sensor response of the PAA/Al multilayer system was compared to the responses of a surface plasmon resonance (SPR) sensor made by a Au thin film on a SF10 glass substrate. It was inferred that the optical waveguide sensor made by the PAA/Al multilayer could detect a smaller change in the refractive index of a solution, and it provided higher resolution than the SPR sensor. The sensor response for a change in the complex refractive index of the PAA layer was examined next, and it was found that the optical waveguide sensor was sensitive to the change in the imaginary part of the complex refractive index rather than the change in the real part. This result indicated that the sensitivity of the optical waveguide sensor could be improved by using the light absorption of a target compound.

Nanoporous films are promising materials as a platform for chemical and biological sensors for two reasons: the large internal surface area of the nanopores allows efficient collection of target compounds into the nanoporous film and the uniform pore diameter, which has molecular dimensions, can be utilized for size-exclusive separation.[1−3] The optical sensing methods for target compounds in nanopores are roughly classified into two approaches, chemical and physical. In the chemical approach, chromogenic or fluorogenic receptor molecules are added into the nanopores to cause selective complexation with target compounds, and then changes in fluorescence or UV−visible absorption are utilized for sensing the target compounds.[4] In the physical approach, changes in optical properties caused by light propagation in the nanoporous film are used to detect target compounds by means of Fabry−Perot fringes,[5,6] photonic band gap (PBG),[7−13] Bragg diffraction,[14] and waveguide mode.[15,16] Since these optical properties are sensitive to the refractive index change of the nanoporous film induced by collection of molecules into the pores, the physical approach can be combined with the chemical approach, that is, changes in optical properties induced by complexation between target compounds or ions and chromogenic or nonchromogenic receptors can be utilized for sensing target compounds. Accordingly, an optical sensor based on a nanoporous thin film is promising for sensing target compounds by the combined use of suitable receptors.

Optical interferometric sensors based on Fabry−Perot fringes have been reported using several nanoporous films, such as a porous anodized silicon film,[5] a mesoporous silica film,[6a] and a mesoporous film of TiO_2−P_2O_5 nanocomposite.[6b,c] When an optically flat nanoporous film has a periodic pore arrangement, PBG can be used as a sensing system, and the PBG sensors based

* To whom correspondence should be addressed. E-mail: teramae@mail.tains.tohoku.ac.jp. Fax: +81-22-795-6549.

(1) Nicole, L.; Boissiére, C.; Grosso, D.; Quach, A.; Sanchez, C. *J. Mater. Chem.* **2005**, *15*, 3598–3627.
(2) Martin, C. R.; Kohli, P. *Nat. Rev. Drug Discovery* **2002**, *2*, 29–37.
(3) (a) Yamaguchi, A.; Uejo, F.; Yoda, T.; Yamashita, T.; Uchida, T.; Tanamura, Y.; Teramae, N. *Nat. Mater.* **2004**, *3*, 337–341. (b) Yamaguchi, A.; Teramae, N. *Anal. Sci.* **2008**, *24*, 25–30. (c) Yamaguchi, A.; Kaneda, H.; Fu, W.; Teramae, N. *Adv. Mater.* **2008**, *20*, 1034–1037.
(4) (a) Lin, V. S.-Y.; Lai, C.-Y.; Huang, J.; Song, S.-A.; Xu, S. *J. Am. Chem. Soc.* **2001**, *123*, 11510–11511. (b) Radu, D. R.; Lai, C.-Y.; Wiench, J. W.; Pruski, M.; Lin, V. S.-Y. *J. Am. Chem. Soc.* **2004**, *126*, 1640–1641.
(5) (a) Lin, V. S.-Y.; Motesharei, K.; Dancil, K.-P. S.; Sailor, M. J.; Ghadiri, M. R. *Science* **1997**, *278*, 840–843. (b) Sohn, H.; Létant, S.; Sailor, M. J.; Trogler, W. C. *J. Am. Chem. Soc.* **2000**, *122*, 5399–5400.
(6) (a) Qi, Z.-M.; Honma, I.; Zhou, H. *App. Phys. Lett.* **2006**, *88*, 053503. (b) Qi, Z.-M.; Honma, I.; Zhou, H. *J. Phys. Chem. B* **2006**, *110*, 10590–10594. (c) Qi, Z.-M.; Honma, I.; Zhou, H. *Anal. Chem.* **2006**, *78*, 1034–1041.
(7) Cunin, F.; Schmedake, T. A.; Link, J. R.; Li, Y. Y.; Koh, J.; Bhatia, S. N.; Sailor, M. J. *Nat. Mater.* **2002**, *1*, 39–41.
(8) Topol'ancik, J.; Bhattacharya, P.; Sabarinathan, J.; Yu, P.-C. *Appl. Phys. Lett.* **2003**, *82*, 1143–1145.
(9) Charlton, C.; Temelkuran, B.; Dellemann, G.; Mizaikoff, B. *Appl. Phys. Lett.* **2005**, *86*, 194102.
(10) Ouyang, H.; DeLouise, L. A.; Miller, B. L.; Fauchet, P. M. *Anal. Chem.* **2007**, *79*, 1502–1506.
(11) (a) Chan, S.; Fauchet, P. M. *Appl. Phys. Lett.* **1999**, *75*, 274–276. (b) Chan, S.; Fauchet, P. M.; Li, Y.; Rothberg, L. J.; Miller, B. L. *Phys. Status Solidi A* **2000**, *182*, 541–546. (c) Chan, S.; Horner, S. R.; Fauchet, P. M.; Miller, B. L. *J. Am. Chem. Soc.* **2001**, *123*, 11797–11798. (d) Ouyang, H.; Christophersen, M.; Viard, R.; Miller, B. L.; Fauchet, P. M. *Adv. Funct. Mater.* **2005**, *15*, 1851–1859.
(12) DeLouise, L. A.; Kou, P. M.; Miller, B. L. *Anal. Chem.* **2005**, *77*, 3222–3230.
(13) Mulloni, V.; Pavesi, L. *Appl. Phys. Lett.* **2000**, *76*, 2523–2525.
(14) Choi, S. Y.; Mamak, M.; von Freymann, G.; Chopra, N.; Ozin, G. A. *Nano Lett.* **2006**, *6*, 2456–2461.
(15) Lau, K. H. A. L.; Tan, L.-S.; Tamada, K.; Sander, M. S.; Knoll, W. *J. Phys. Chem. B* **2004**, *108*, 10812–10818.
(16) Qi, Z.-M.; Honma, I.; Zhou, H. *Appl. Phys. Lett.* **2007**, *90*, 011102.

10.1021/ac8015642 CCC: $40.75 © 2009 American Chemical Society
Published on Web 12/02/2008

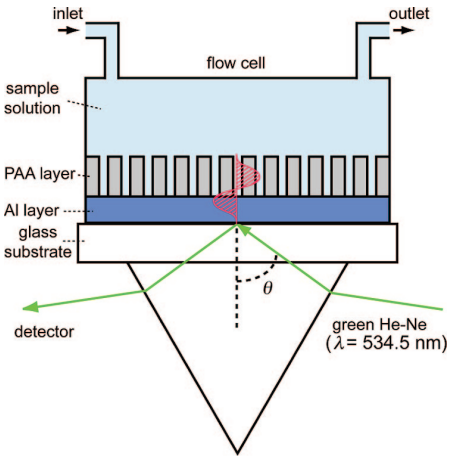

Figure 1. Schematic of the optical waveguide sensor setup and of the idealized field distribution of a single guided mode.

on porous anodized silicon films have also been reported.[7−10] Mesoporous Bragg stack color-tunable sensors reported by Choi et al.[14] are based on mesoporous Bragg stacks composed of multilayer stacks of mesoporous TiO_2 and mesoporous SiO_2. There are microcavity sensors based on a one-dimensional PBG structure that contain a central sensing layer sandwiched by two Bragg mirrors, and they have been fabricated by anodization of silicon substrates.[11−13] The optical waveguide sensors made by nanoporous and metallic multilayer films show a waveguide coupling dip, and the sensor response is based on the dip shift caused by the changes in the refractive index of the nanoporous layer.[15,16]

In the present study, a porous anodized alumina (PAA) and Al (PAA/Al) multilayer film was fabricated and its application as an optical waveguide sensor was studied. Figure 1 shows a schematic illustration of the optical waveguide spectroscopy setup and the idealized field distribution of a single guided mode. When a nanoporous and metallic multilayer on a glass substrate is irradiated with light under the Kretschmann configuration, optical waveguide modes can be excited in the nanoporous film, and a sharp and deep waveguide coupling dip appears in the angular spectrum.[17−19] Since the position of the waveguide coupling dip is sensitive to the refractive index of the nanoporous film, the signal transduction can be monitored by a shift of the waveguide coupling dip. Until now, several attempts have been made to fabricate nanoporous film waveguides: a porous anodic alumina film on a Au thin film,[15] and a nanoporous TiO_2 film, which is composed of aggregated colloidal TiO_2 particles, on a Au thin film.[16] These nanoporous film waveguides showed sharp and deep dips in their angular spectra (dependence of reflectivity on the incident angle of light), and the shift of the dip position was utilized for detection of bovine serum albumin,[15] myoglobin,[15] and NH_3 gas.[16] These optical waveguide sensors are made by a nanoporous film on a Au layer. In contrast, here we attempted to form the PAA layer on the Al layer instead of the Au layer because the PAA/Al multilayer can be simply fabricated by an anodization of the Al film on a glass substrate.

(17) Welford, K. *Opt. Quantum Electron.* **1991**, *23*, 1–27.
(18) Osterfeld, M.; Franke, H.; Feger, C. *Appl. Phys. Lett.* **1993**, *62*, 2310–2312.
(19) Knoll, W. *Annu. Rev. Phys. Chem.* **1998**, *49*, 569–638.

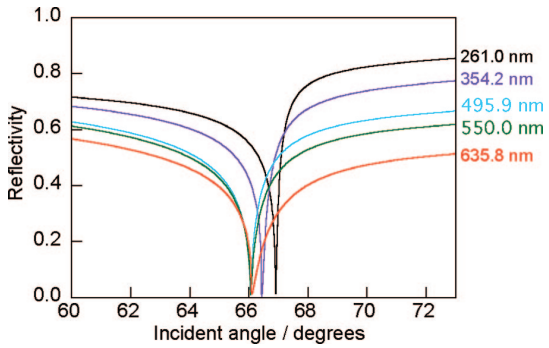

Figure 2. Fresnel calculations of angular spectra for the water/nonporous alumina/Al/quartz multilayer system. Optical constants used for the Fresnel calculations are summarized in Table 1.

In addition, the use of the Al layer under the PAA layer allows the appearance of a clear waveguide coupling mode from UV to visible wavelength regions (see Figure 2). Since the optical waveguide coupling mode is sensitive to the light absorption behavior of target compounds distributed inside the alumina pore as confirmed in this study, there is a possibility to utilize light absorption of a target compound from UV to visible regions for the response of an optical waveguide sensor made by the PAA/Al multilayer film.

This paper consists of four parts to illustrate the availability of the PAA/Al multilayer film for a sensitive optical sensor: (1) Fresnel calculation of optical waveguide mode with different wavelengths of monitoring light; (2) fabrication and characterization of the PAA/Al multilayer film on a glass substrate; (3) sensor response for liquid samples with different refractive indices; and (4) sensor response induced by the changes in the imaginary part of the complex refractive index of the PAA layer. First, we discuss the available wavelength region of monitoring light for the optical waveguide sensor based on the PAA/Al multilayer film by Fresnel calculation. Second, since the shape of the waveguide mode depends strongly on the thickness of the PAA layer, the preferable layer thickness is examined to obtain a sharp and deep dip by considering the structure of the PAA/Al multilayer film characterized by scanning electron microscopy (SEM) and transmission electron microscopy (TEM) measurements. Third, the shift of the waveguide coupling dip found for the PAA/Al multilayer film as a function of refractive indices of the adjacent solution phases is discussed. The experimental results show that the position of the waveguide coupling dip shifts toward a higher incident angle as the refractive index of the solution (water-ethanol mixture) increases. The PAA/Al multilayer film system is sensitive to the change in the refractive index of the water-ethanol mixture solution, and its sensitivity is higher than that of a surface plasmon resonance (SPR) sensor made by a Au thin film on a glass substrate. Finally, we examine sensor responses of the PAA/Al multilayer film system toward changes in the complex refractive index of the PAA layer, and we confirm that the sensor response is sensitive to the change of the imaginary part of the complex refractive index rather than that of the real part. The results presented in this paper verify that the optical waveguide sensor made by the PAA/Al multilayer film has a potential sensing ability with high sensitivity.

Table 1. Optical Constants Used for Fresnel Calculations shown in Figure 2

	261.0 nm	354.2 nm	495.9 nm	550.0 nm	635.8 nm
alumina[a]	1.8358	1.7963	1.7744	1.7702	1.7657
quartz[b]	1.5003	1.4763	1.4624	1.4597	1.4567
Al[d]	0.209 + 3.11i	0.385 + 4.30i	0.755 + 6.03i	0.958 + 6.69i	1.39 + 7.65i
water[c]	1.3800	1.3530	1.3365	1.3341	1.3314
aluminum thickness	82 nm	123 nm	180 nm	204 nm	242 nm
Al thickness	21 nm	20 nm	17 nm	16 nm	14 nm

[a] Reference 22. [b] Refractive index list for fused quartz from Sigma-Koki Co. Ltd. (Japan). [c] Reference 23. [d] Reference 24.

EXPERIMENTAL SECTION

Materials. Square cover glasses (25 × 25 × 0.3 mm^3; Matsunami Glass Ind., Ltd., Osaka, Japan) were used as substrates on which the PAA/Al multilayer film was formed. Al wire (99.99%; Nilaco Co., Tokyo, Japan) was used for the thermal deposition of Al films. Milli-Q water was used for all experiments. All organic solvents and chemical reagents were purchased from Wako Pure Chemical Industries Ltd. (Osaka, Japan) and were used as-received.

Fabrication of PAA/Al Multilayer Film. The glass substrate was sonicated in acetone, methanol, and water for 5 min each. Then it was immersed in concentrated nitric acid and boiled at 100 °C for 1 h to remove organic species adsorbed on the substrate surface. Next, its surface was etched by immersing it in a 10 wt % hydrofluoric acid solution for 30 s. After rinsing the glass substrate with water and drying it under a nitrogen gas stream, an Al film was deposited on the glass substrate using a Ulvac model VPC-1100 vacuum deposition system. The thickness of the Al film was measured by a Tencor Alpha-Step 500 surface profiler.

The anodizing of the Al film was carried out at a constant potential according to the literature[20] with some modifications; the constant potential of 30 V was applied to the film while immersed in a 0.5 M oxalic acid solution at 5 °C. After a few minutes, the film color became green and transparent, indicating the formation of a PAA/Al multilayer film (Figure 3A). The film color was monitored by the naked eye, and the time to stop the anodizing was decided accordingly. Then, the resulting PAA/Al multilayer film was washed thoroughly with water and dried in air. It should be emphasized that the reproducibility of fabricating the PAA/Al multilayer films with the same optical properties was about 80%.

The structure of the PAA/Al multilayer film was characterized by SEM and TEM. The SEM measurements were performed on a Field-Emission SEM (Hitachi; S-4300, or JEOL; JFC-1200). The TEM measurements were performed on a JEM-200EX (JEOL) equipped with a field emission gun operated at 200 kV. To prepare samples for TEM cross-sectional views, the substrate was embedded in an epoxy resin and cut orthogonally to the sample surface. Then it was treated by mechanical polishing, dimpling, and argon ion milling.

Optical Waveguide Spectroscopy. Optical waveguide spectroscopy was carried out using the Kretschmann prism coupling technique,[15] and reflectivity was measured as a function of incident angle (angular spectrum) using a green He−Ne laser (534.5 nm, 1 mW) as a light source. The laser beam was modulated by an NF model CH-353 light chopper at 733 Hz. A Fresnel rhomb and a polarizer were used to form p-polarized light. The sample substrate was attached to a BK7 equilateral dispersing prism via an index matching fluid (Cargille; immersion oil No. 16242), and the substrate was irradiated by p-polarized light. The intensity of reflected light was detected by a Hamamatsu model S2281 Si photodiode, and the signal was processed by an NF model 5610B lock-in amplifier. An analyzer was placed in front of the Si photodiode to detect p-polarized reflection light. The reflectivity of the PAA/Al multilayer film was normalized using the intensity of reflection light observed for a bare glass substrate attached to the BK7 prism via the index matching fluid.

The above optical setup was also used to measure the SPR response of the Al layer deposited on the glass substrate. The observed SPR reflectivity curve (reflectivity vs incident angle) of the Al layer was used to estimate the complex refractive index of the Al layer.[21] In this measurement, the sample glass substrate with an Al layer was attached to the equilateral dispersing prism

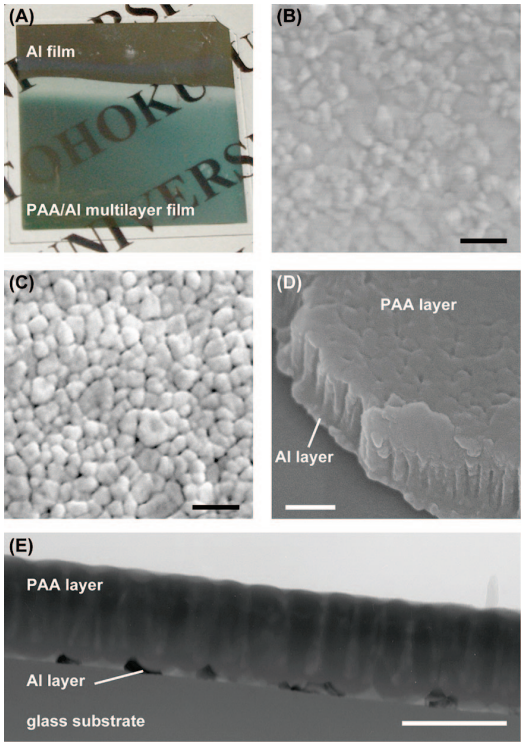

Figure 3. (A) Photograph of the Al film on the glass substrate after anodization. SEM top views of (B) an Al film before anodization and (C) a PAA layer after anodization. (D) SEM cross-sectional view of the PAA/Al multilayer film on a glass substrate. (E) TEM cross-sectional view of the PAA/Al multilayer film. Scale bars corresponds to 200 nm.

(20) Masuda, H.; Satoh, M. *Jpn. J. Appl. Phys.* **1996**, *35*, L126–L129.

(BK7) via the index matching fluid. The refractive indices of solution phases (water and water-ethanol mixtures) were estimated by measuring the critical angle at the interface between the solution and the glass substrate. The critical angle was measured by attaching a bare glass substrate to the equilateral dispersing prism (BK7) via the index matching fluid.

RESULTS AND DISCUSSION

Fresnel Calculation of Angular Spectra with Different Wavelengths of Monitoring Light. To determine the optimum wavelength of monitoring light, angular spectra for different light wavelengths were simulated by the four-phase Fresnel calculation for water/nonporous alumina/Al/quartz system. Since the refractive indices of nonporous alumina and quartz have been well-known, nonporous alumina and quartz were used instead of PAA and cover glass, respectively (Table 1). For the Fresnel calculations, the complex refractive indices of Al in the literature[23] were used, and the refractive indices of water, nonporous alumina, and quartz were obtained by the best fit of data given in the references[22,24] to Cauchy's equation ($n = n_0 + n_1/\lambda^2 + n_2/\lambda^4$). The thicknesses of each layer were adjusted to show a sharp and deep waveguide coupling dip. As shown in Figure 2, a clear waveguide coupling dip can be obtained by the simulations using monitoring light of the UV to visible wavelength regions. These simulations suggest that wavelength of monitoring light can be chosen from UV to visible regions for an optical waveguide sensor made by PAA/Al multilayer film if remarkable absorption and scattering of monitoring light within a PAA layer and a cover glass substrate do not occur. In this study, a metal complex with an absorption band around 510 nm was distributed inside the PAA layer to examine the effect of light absorption occurring inside the PAA layer. Accordingly, we chosed the green He−Ne laser (534.5 nm) as a light source in this study.

Structure of the PAA/Al Multilayer Film. The SEM and TEM images of the PAA/Al multilayer film, which was prepared by anodizing the Al film with a thickness of 180 nm, are shown in Figure 3. The SEM top views (Figure 2B,C) reveal that anodizing of the Al film results in the formation of a PAA layer with pores of about 20 nm in diameter. From the TEM cross-sectional view (Figure 3E), the pores in the PAA layer can be recognized to have a columnar structure; this is commonly observed for the PAA layer.[20] In this TEM image, defects in the Al layer are also recognized, and the Al layer seems to be island-like. However, such defects in the Al layer are not observed in the cross-sectional SEM images of the PAA/Al multilayer film on the glass substrate after cleavage (Figure 3D). Hence, the defects might be formed during ion-milling in the sample preparation for the TEM observation. The average thicknesses of the PAA and the Al layers were estimated from the TEM images and are about 200 nm for the PAA layer and about 17 nm for the Al layer. The porosity of the PAA layer was estimated from the analysis of the SEM top view by using image processing software (Mitani; WinRoof),[25] and the value is about 7%.

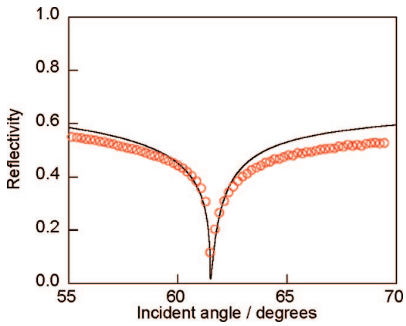

Figure 4. Angular spectrum observed for the PAA/Al multilayer film. The thickness of the PAA and Al layers are 200 and 17 nm, respectively. The solid line is an angular spectrum simulated by the Fresnel calculation using the following parameters: 17 and 200 nm for the thicknesses of the Al and PAA layers, and 1.519, 1.00 + 5.97i, 1.77, and 1.335 for the refractive indices of the glass substrate, Al layer, PAA layer, and water, respectively.

Angular Spectrum of PAA/Al Multilayer Film. The angular spectrum (reflectivity vs incident angle) of the PAA/Al multilayer film, whose structures are shown in Figure 3, was measured in water, and the observed spectrum was compared to the spectrum simulated by the Fresnel calculation (Figure 4). The simulated spectrum exhibits a waveguide coupling dip with the first order mode, and the coupling angle is around 61.51°. The spectral shapes of the observed and the simulated spectra agree well with each other, indicating that the dip in the observed angular spectrum is ascribed to the waveguide coupling dip and that the PAA/Al multilayer fabricated in this study exhibits a well-defined optical waveguide mode.

For the Fresnel calculation, the refractive index of the Al layer (1.00 + 5.97i) was determined by measuring the SPR reflectivity curve of the Al layer on the glass substrate, and the thicknesses of the PAA and the Al layers were estimated from the SEM and the TEM images. The refractive index of the PAA layer was assumed as 1.77 because the angular spectrum calculated by using this refractive index value agrees well with the observed spectrum (Figure 4). The refractive index of amorphous alumina is reported as 1.77 at 534.5 nm.[21] In general, the refractive index of a porous material is smaller than that of a nonporous one.[15] Accordingly, the refractive index of the PAA layer must be smaller than that of porous alumina. However, both refractive indices are comparable, which can be ascribed to the low porosity (ca. 7%) of the PAA layer used in this study.

Optimization of the PAA Thickness. From the Fresnel calculation for the PAA/Al multilayer film systems, we confirmed that the sharpness and deepness of the waveguide coupling dip depend strongly on the physical properties of the PAA layer rather than the Al layer. Hence, we simulated the effect of the PAA layer thickness on the shape of the waveguide coupling dip by keeping the Al thickness as 17 nm. As shown in Figure 5B, the PAA layer thickness of 200 nm provides the sharpest and deepest waveguide coupling dip (spectrum *a*) compared to other PAA layers with

(21) de Byuijn, H. E.; Koovman, R. P. H.; Greve, J. *Appl. Opt.* **1990**, *29*, 1974–1978.
(22) Gervais, F. In *In Handbook of Optical Constants of Solids II*; Palik, E. D., Ed,; Academic Press, Inc.: Orlando, 1991; pp 761−775.
(23) Smith, D. Y.; Shiles, E.; Inokuti, M. In *Handbook of Optical Constants of Solids*; Palik, E. D., Ed.; Academic Press, Inc.: Orlando, 1985; pp 369−406.
(24) RothW. A. ScheelK. *Landolt Börnstein Tabelen*, 5 Auflage; Springer-Verlag: Berlin, 1931; p 966.
(25) Yamaguchi, A.; Yoda, T.; Suzuki, S.; Morita, K.; Teramae, N. *Anal. Sci.* **2006**, *22*, 1501–1507.

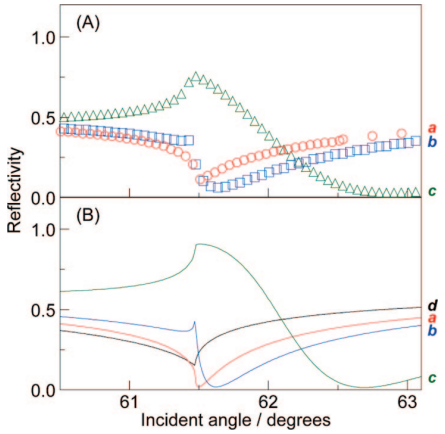

Figure 5. (A) Observed angular spectra of PAA/Al multilayer films prepared by partial anodization of Al films with different initial thicknesses: the initial thicknesses of Al films are 180 nm, 190 nm, and 200 nm for spectra *a* (open circles), *b* (open squares), and *c* (open triangles), respectively. (B) Angular spectra of PAA/Al multilayer films simulated by the Fresnel calculation: thicknesses of PAA layers are 190 nm, 200 nm, 205 nm, and 222 nm for spectra *d*, *a*, *b*, and *c*, respectively; the refractive indices of the glass substrate, Al layer, PAA layer, and water are 1.519, 1.00 + 5.97i, 1.77, and 1.335, respectively.

different thicknesses. When the PAA thickness is larger than 200 nm, the waveguide coupling angle shifts toward higher values, and the dip around the waveguide coupling angle is broadened as typically shown in spectra *b* and *c* of Figure 5B. When the PAA thickness is smaller than 200 nm, the position and sharpness of the waveguide coupling dip are almost the same as the case of the thickness of 200 nm, whereas the dip typically becomes shallow as shown in spectrum *d* of Figure 5B. Considering the sensing application, it is preferable that the waveguide coupling dip be sharp and deep. Therefore, these simulation results strongly indicate the necessity of regulating the thickness of the PAA film at around 200 nm.

In our fabrication procedure for the PAA/Al multilayer film, the PAA thickness can be regulated by controlling the vacuum evaporation time to form the Al film preceding the anodization, and the anodizing of a thicker Al film results in a thicker PAA layer. Hence, three Al films with different thicknesses were fabricated and anodized to compare the waveguide coupling efficiency. Swelling of the PAA layer because of anodization causes the total thickness of the PAA/Al layer to become larger compared to the initial Al layer. Figure 5A shows angular spectra of the PAA/Al multilayer films with different initial thicknesses of Al film. Spectrum *a* in Figure 5A was measured for the PAA/Al multilayer film for which the initial thickness of the Al film was 180 nm and the thickness of the PAA layer was 200 nm after anodization. This spectrum is the same as that in Figure 4. The formation of a PAA layer thicker than 200 nm occurs by anodizing the Al film with a thickness of 190 nm. Spectrum *b* shows a shift of the waveguide coupling angle and broadening of the dip compared to spectrum *a*. The PAA/Al multilayer film prepared by anodizing the Al film with a thickness of 200 nm shows a further shift of the waveguide coupling angle and also further broadening (spectrum *c*). From these results, we conclude that anodizing of the Al film with an initial thickness of 180 nm is suitable for the preparation of a PAA/Al multilayer film that exhibits a clear waveguide coupling dip.

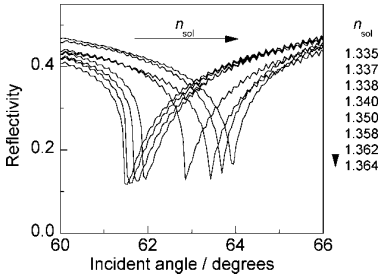

Figure 6. Angular spectra of the PAA/Al multilayer film observed for solutions with different refractive indices (n_{sol}).

Optical Waveguide Mode Dependence on the Refractive Index of a Solution Phase. Dependence of the optical waveguide mode on the refractive index of a solution phase was examined next. Figure 6 shows angular spectra of water/ethanol mixtures with different refractive indices. The refractive indices of the water/ethanol mixtures were changed by varying the composition ratio of water and ethanol, and the values of refractive indices were determined by the critical angle measurements. The waveguide coupling angle (θ_{WCA}) shifts to higher values with increasing refractive index (n_{sol}) of the solution phase, and the difference of θ_{WCA} ($\Delta\theta_{WCA}$) between the lowest (1.335) and the highest (1.364) refractive indices of the solution phase is 2.43° (see Figure 7B). When the θ_{WCA} shift is calculated for the nonporous alumina/Al multilayer system, the θ_{WCA} shift depending on the refractive index of a solution between 1.335 and 1.364 is 2.36°, and this value is slightly smaller than that found in the PAA/Al multilayer system. Hence, although the observed angle shift would be mainly due to the change in the refractive index of bulk solution phase, the refractive index change of the PAA layer might also contribute to the angle shift similarly to the PAA/Au multilayer system reported by Lau et al.[15] The pores of the PAA layer are filled with the solution, and a change in the solution composition would cause the change in refractive indices inside and outside the PAA layer, which contributes to the shift of the waveguide coupling angle.

To discuss the sensitivity toward changes in n_{sol}, the Fresnel calculation was carried out to simulate SPR reflectivity curves for a Au thin film on an SF10 glass substrate (Au/SF10). In general, the SPR dip becomes narrower for longer wavelengths of monitoring light, and the wavelength around 800 nm has been usually used to develop a sensitive SPR sensor made by Au/SF10.[26–28] As reported by Nelson et al.,[27] experimental SPR reflectivity curves (angular spectra) agree well with the theoretical curves simulated by Fresnel calculation. Figure 7A shows the angular spectrum for the Au/SF10 simulated using optical constants (Au thin film: $n^{\wedge} = 0.165 + 5.205i$, SF10: $n = 1.711$) and the thickness of Au thin film (45.0 nm) given in the literature[27]

(26) Nelson, B. P.; Grimsrud, T. E.; Liles, M. R.; Goodman, R. M.; Corn, R. M. *Anal. Chem.* **2001**, *73*, 1–7.
(27) Nelson, B. P.; Frutos, A. G.; Brockman, J. M.; Corn, R. M. *Anal. Chem.* **1999**, *71*, 3928–3924.
(28) Homola, J. *Sens. Actuators B* **1997**, *41*, 207–211.

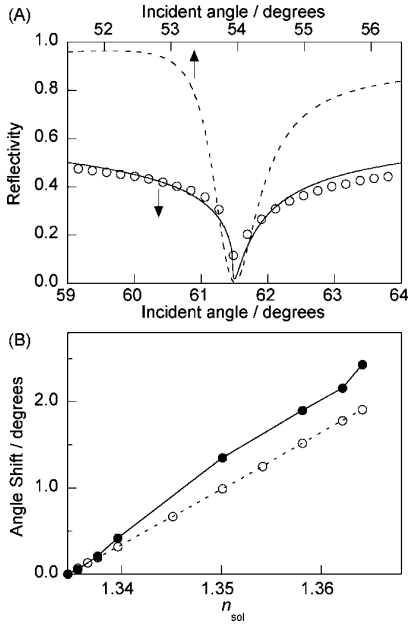

Figure 7. (A) Comparison of angular spectra for the optical waveguide sensor made by PAA/Al multilayer film (open circles) and the SPR sensor based on Au/SF10 (dashed line). Optical constants for the Au/SF10 are from ref 26 (Au thickness, 45 nm; refractive index of Au, 0.165 + 5.205i; refractive index of SF10, 1.711; wavelength of light, 814 nm). The refractive index of the solution is 1.3346 (pure water). (B) Shift of waveguide coupling angle for the PAA/Al multilayer film and shift of SPR angle for Au/SF10 depending on the solvent refractive index (n_{sol}). The SPR angles were calculated by using above optical constants for Au/SF10.

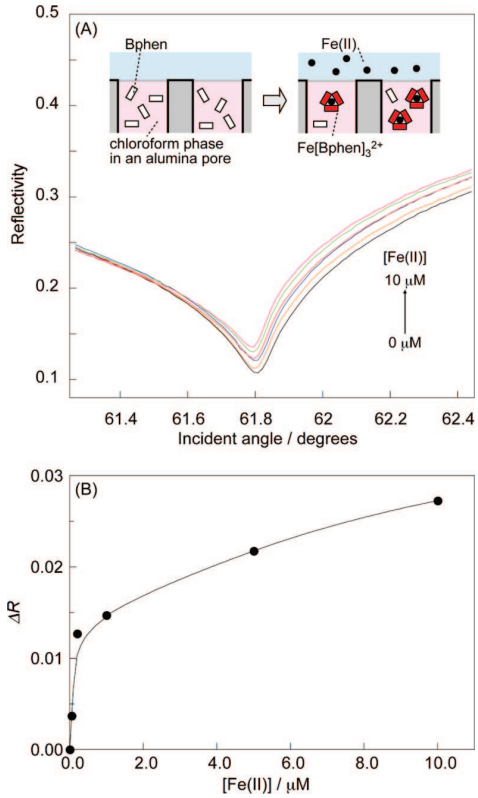

Figure 8. (A) Angular spectra of the PAA/Au multilayer film in contact with a Fe(II) solution in the flow cell. (B) Reflectivity change (ΔR) at the waveguide coupling dip (incident angle = 61.81°) vs the Fe(II) concentration.

at the wavelength (814 nm) of the monitoring light. The angular spectrum for the present optical waveguide sensor (PAA/Al) is also shown for comparison. As shown in Figure 7A, we can recognize that the waveguide coupling dip for the PAA/Al multilayer film is narrower than the SPR dip for the Au/SF10. Angle shifts of the waveguide coupling dip and SPR dip were also simulated by changing the refractive index of a solution, and the results are shown in Figure 7B. The shift of the waveguide coupling angle for the solution refractive index change between 1.335 and 1.364 is slightly larger than the SPR angle shift. The narrower waveguide coupling dip indicates that the waveguide coupling angle can be determined with higher resolution than the SPR angle. The slightly larger angle shift suggests that the position of the waveguide coupling angle is slightly sensitive compared to that of the SPR angle. Accordingly, we infer from the comparison of the waveguide coupling angle shift and the SPR angle shift that the present waveguide sensor made by the PAA/Al multilayer film is sensitive to the change in the refractive index of a solution phase, and its sensitivity is higher than that of a SPR sensor made by Au/SF10.

Lau et al.[15] fabricated a PAA/Au multilayer film and applied it as an optical waveguide sensor. The angle shift $\Delta\theta_{WCA}$ of their sensor was 0.92° for the change in the refractive index of a solution from 1.332 (phosphate buffer) to 1.358 (pure ethanol). In the present study, the $\Delta\theta_{WCA}$ is 1.9° for the change in the refractive index of a solution from 1.335 to 1.358, and this value is 2.1 times larger than the reported one.[15] Accordingly, the present optical waveguide sensor made by the PAA/Al multilayer film might be said to have better sensitivity than the sensor based on the PAA/Au multilayer film reported by Lau et al.[15]

Optical Waveguide Mode Dependence on the Complex Refractive Index of the PAA Layer. If light-absorbing species are present in the PAA layer of the optical waveguide sensor, the sensor response must be described using the complex refractive index whose imaginary part is related to the light absorption. To examine the sensor response according to the change in the imaginary part of the complex refractive index of the PAA layer, bathophenanthroline (Bphen) was distributed into the PAA layer and its complex formation with Fe(II) was monitored. Since $Fe[Bphen]_3^{2+}$ shows a broad absorption band centered at around 510 nm which is close to the wavelength of the monitoring light (534.5 nm) used in this study, the formation of $Fe[Bphen]_3^{2+}$ within the PAA layer can cause a change in the complex refractive index of the PAA layer. The experiment was performed as shown in Figure 8 A. First, the inner walls of the alumina pores were modified with dichlorodimethylsilane by immersing the sample substrate in a dichlorodimethylsilane-ethanol mixture (2 wt %) for 2.5 h. Then, the sample substrate was set in a flow cell, and the alumina pores were filled with chloroform. Bphen was then distributed into the chloroform phase inside the alumina pores by passing a Bphen-saturated aqueous solution (also saturated with chloroform) through the flow cell. After washing the flow cell to remove the Bphen that remained

in it, a sample solution containing Fe(II) was introduced into the flow cell. While the Fe(II) solution was flowing, $Fe[Bphen]_3^{2+}$ was formed and distributed into the chloroform phase inside the alumina pores. Constituents of the sample solution were Fe(II), acetate buffer (265 mM, pH 4.97), hydroxylamine (58 mM), and sodium perchlorate (200 mM). The concentration of Fe(II) ranged from 50 nM to 10 μM. Because of the presence of hydrophobic perchlorate, the distribution of $Fe[Bphen]_3^{2+}$ into the chloroform phase is enhanced because of the formation of an ion-pair between perchlorate ions and $Fe[Bphen]_3^{2+}$.[29] Under the present experimental conditions, the amount of $Fe[Bphen]_3^{2+}$ in the aqueous solution phase is negligibly small, and the amount of $Fe[Bphen]_3^{2+}$ within the PAA layer can be varied by changing the concentration of Fe(II). Therefore, we can examine the effect of the complex refractive index of the PAA layer on the waveguide coupling mode by keeping the complex refractive index of the solution phase as a constant.

Figure 8A shows the observed angular spectra. In the absence of Fe(II), θ_{WCA} is 61.81°, and this value is shifted from that observed for pure water (see Figure 4) because of the presence of ionic species in the sample Fe(II) solution. By introducing a sample solution containing Fe(II) into the flow cell, reflectivity around the waveguide coupling dip remarkably increases with increasing concentration of Fe(II) as shown in Figure 8B, whereas the shift of θ_{WCA} is not significant. It should be mentioned that the optical waveguide sensor made by the PAA/Al multilayer film exhibited no remarkable changes in its angular spectra when the Fe(II) solutions were introduced into the flow cell without the distribution of Bphen into the chloroform phase inside the alumina pores, indicating that the reflectivity change shown in Figure 8 is due to the formation and distribution of $Fe[Bphen]_3^{2+}$ into the chloroform phase inside the alumina pores. The absorption maximum of $Fe[Bphen]_3^{2+}$ in an aqueous solution is around 510 nm and the distribution of $Fe[Bphen]_3^{2+}$ into the chloroform phase inside the PAA pores causes a change in the complex refractive index of the PAA layer. On the basis of the Fresnel calculation, we conclude that the increase in the imaginary part of the complex refractive index of the PAA layer mainly induces an increase in the reflectivity at around the waveguide coupling dip and that an angle shift of θ_{WCA} is mainly caused by an increase in the real part. Hence, the result shown in Figure 8 suggests that the optical waveguide sensor made by the PAA/Al multilayer film is sensitive to the change in the imaginary part of the refractive index of the PAA layer rather than the change in the real part. The utilization of light absorption of a target compound will improve the response of the optical waveguide sensor as similarly seen for the absorption-based SPR sensor.[30]

(29) Radhakrishnan, L.; Yamaguchi, A.; Fu, W.; Kaneda, H.; Teramae, N. *Microporous Mesoporous Mater.* **2008**, *113*, 139–145.

CONCLUSION

In the present study, the PAA/Al multilayer film on a glass substrate was developed by a partial anodization of an Al film, and its potential application as an optical waveguide sensor was demonstrated. For the fabrication of the PAA/Al multilayer film on a glass substrate, we confirmed that the initial thickness of Al film strongly influenced the shape of the waveguide coupling dip and that an initial thickness of 180 nm was suitable to get a deep and sharp optical waveguide coupling dip. The optical sensor response of the PAA/Al multilayer system was compared to the response of an SPR sensor made by a Au thin film on SF10 glass substrate. We inferred that the present optical waveguide sensor could detect a small change in the refractive index of a sample solution and that the present sensor showed higher resolution than the SPR sensor. Moreover, it was confirmed that the present optical waveguide sensor was sensitive to the change in the imaginary part of the complex refractive index rather than the real part. The results on the detection of $Fe[Bphen]_3^{2+}$ indicated that using light absorption of a target compound could improve the sensitivity of the optical waveguide sensor. Since the Fresnel calculation predicted that a clear waveguide coupling dip would appear for monitoring light ranging from the UV to visible regions, this strongly indicated that the optical waveguide sensor made by the PAA/Al multilayer film could be used to detect a variety of chemical species which show absorptions from UV to visible regions.

ACKNOWLEDGMENT

This work was supported in part by Grants-in-Aid for Scientific Research (No. 17205009 and No. 18750058) from the Ministry of Education, Culture, Sports, Science and Technology, Japan, and by Precursory Research for Embryonic Science and Technology (PRESTO), Japan Science and Technology Agency (JST). We acknowledge Mr. Masaki Okude and Dr. Akira Ohtomo, Institute for Materials Research, Tohoku University, for measuring the thicknesses of Al films deposited on glass substrates. We also acknowledge Dr. Tsunenobu Onodera, Institute of Multidisciplinary Research for Advanced Materials (IMRAM), Tohoku University, for SEM measurement.

Received for review July 24, 2008. Accepted November 10, 2008.

AC8015642

(30) (a) Kurihara, K.; Suzuki, K. *Anal. Chem.* **2002**, *74*, 696–701. (b) Kurihara, K.; Nakamura, K.; Hirayama, E.; Suzuki, K. *Anal. Chem.* **2002**, *74*, 6323–6333.